ADVANCED MATERIALS
www.advmat.de

Shine Bright Like a Diamond: New Light on an Old Polymeric Semiconductor

Paolo Giusto, Daniel Cruz, Tobias Heil, Hiroki Arazoe, Paola Lova, Takuzo Aida, Davide Comoretto, Maddalena Patrini, and Markus Antonietti**

Brilliance usually refers to the light reflected by the facets of a gemstone such as diamond due to its high refractive index. Nowadays, high-refractive-index materials find application in many optical and photonic devices and are mostly of inorganic nature. However, these materials are usually obtained by toxic or expensive production processes. Herein, the synthesis of a thin-film organic semiconductor, namely, polymeric carbon nitride, by thermal chemical vapor deposition is presented. Among polymers, this organic material combines the highest intrinsic refractive index reported so far with high transparency in the visible spectrum, even reaching the range of diamond. Eventually, the herein presented deposition of high quality thin films and their optical characteristics open the way for numerous new applications and devices in optics, photonics, and beyond based on organic materials.

Semiconductor materials are among the most important materials in research and industrial applications. They are widely used in electronic, optoelectronic, and photonic devices such as transistors, solar cells, and optical sensors. Despite recent developments, inorganic semiconductors like silicon still play a major role. Yet, they reach their limits, e.g., because of toxic and expensive production processes or missing mechanical flexibility hindering their application in wearables or biological systems. Polymeric semiconductors are a promising class of materials that can overcome these problems in order to develop new generation devices which are more efficient, flexible, cost-effective, and sustainable. However, current polymeric semiconductors are mostly disordered 1D polymers, which require the optimization of both intra- and intermolecular electron transport. Furthermore, molecular effects as well as packing have to be taken into account. In contrast, 2D polymers such as graphene can be controlled and processed much easier. Among the 2D structures, polymeric carbon nitride (pCN) has attracted much attention in the last decade due to its high thermal stability and unique electronic properties, which have been widely exploited for photocatalysis with visible light.[1,2] The pCN materials have a long history, almost as old as synthetic organic chemistry.[3] In 1834, Berzelius and Liebig reported the first synthesis of a polymeric carbon nitride and named the product melon. Eventually, pCN is one of the oldest published synthetic polymers.[4] However, up to now, broader applications as electronic semiconductors were restricted by the limited processability, as the product is neither soluble nor malleable.[5] As a consequence, pCN thin films cannot be prepared by common solvent-based methods such as spin-coating, spray-coating, or inkjet printing.[6] Furthermore, current films are mostly opaque, rough, and particulate with defects, and therefore currently far from the quality of inorganic semiconductors.[6–8] Eventually, also the application of pCN in photonics and optoelectronics has been explored only little as it requires the preparation of highly homogeneous thin films with tunable thickness and constant structural order in the nanometer range.

Methods for the thin film deposition of pCN have recently been addressed by different gas-phase techniques which, however, still suffer from poor deposition quality, i.e., low homogeneity and/or high roughness.[6,8] Due to the promising characteristics and the potential to significantly drive innovation, a synthesis of pCN thin films is strongly required. Recently, Aida and co-workers were first to produce transparent pCN coatings.[9] Unfortunately, the films underwent swelling, bending, and delamination, which indicates still incomplete condensation as well as film inhomogeneity such as structure gradients in growth direction.

Inspired by these groundbreaking results, we decided to improve deposition conditions by means of chemical vapor

P. Giusto, D. Cruz, Dr. T. Heil, Prof. M. Antonietti
Department of Colloid Chemistry
Max Planck Institute of Colloids and Interfaces
Am Mühlenberg 1, 14476 Potsdam, Germany
E-mail: Paolo.Giusto@mpikg.mpg.de; office.cc@mpikg.mpg.de
Dr. H. Arazoe, Prof. T. Aida
Department of Chemistry and Biotechnology
School of Engineering
The University of Tokyo
Tokyo 113-8656, Japan
Dr. P. Lova, Prof. D. Comoretto
Dipartimento di Chimica e Chimica Industriale
Università degli Studi di Genova
Via Dodecaneso 31, 16146 Genova, Italy
Prof. M. Patrini
Department of Physics
University of Pavia
Via Bassi, 6, 27100 Pavia, Italy
The ORCID identification number(s) for the author(s) of this article can be found under https://doi.org/10.1002/adma.201908140.

DOI: 10.1002/adma.201908140

deposition (CVD). As a result, we herein present a deposition method to obtain transparent, highly homogeneous pCN thin films over large surfaces with tunable nanothickness from a low-cost commodity solid precursor, i.e., melamine. These pCN thin films derived by CVD possess a highly oriented and conjugated layered structure with intense blue fluorescence as well as a very high intrinsic refractive index (n) in the visible range, which, to the best of our knowledge, is the highest value reported so far for polymeric materials, accompanied by high optical transparency in the visible range.[10,11] These values lie even in the range of diamond, which has the highest refractive index for carbon-based materials, and is commonly known to be the most brilliant material of all.[12] Such high n thin films are of paramount importance not only for light harvesting nanostructured systems and optical light trapping but also for the development of highly efficient optical nanodevices such as Mie resonators, photonic crystals, optical fibers, and optical sensors.[13,14]

Melamine is a well-known solid precursor for the synthesis of pCN, which is of low toxicity, cheap, and available in high quantities. Melamine conveniently sublimes at relatively low temperatures (Figure S1, Supporting Information).[15] Eventually, in order to achieve high-quality thin film deposition, a double zone thermal CVD setup was used. Here, the melamine precursor sublimes in the first zone and polymerizes on a substrate surface in the second zone at 550 °C (**Figure 1**a,b). As shown by the pCN films deposited on a fused silica wafer and on a flower-shaped quartz substrate (Figure 1c–f), the pCN deposition occurs homogeneously over large surface areas of up to 2 in. in diameter and without constraints on the substrate shape. Moreover, the pCN thin film thickness can be successfully tuned within a wide range by placing different amounts of melamine precursor in the sublimation zone and/or by changing the synthesis time. It is worth to point out, that the melamine precursor is completely sublimated during the deposition process thus allowing for precise control over the deposition parameters. The obtained pCN thin films are usually crack-free and reveal a very low average surface roughness (<2 nm Rq) over surfaces of 100 μm^2, basically equal to the bare substrate as confirmed by atomic force microscopy (AFM) (Figure S2a,b, Supporting Information). The low surface roughness is an important parameter to avoid undesired scattering effects that can be detrimental for photonic applications.

The quality of the deposited pCN thin films at the microscale was investigated by scanning electron microscopy (SEM). The films appear highly homogeneous and crack-free over large surfaces: the homogeneity is so high that is even difficult to say whether the film is present or not, on flat as well as curved edges (Figure S3a,b, Supporting Information). The presence of the pCN thin film is, however, confirmed by energy-dispersive X-ray analysis (EDX) elemental mapping of carbon, nitrogen, silicon, and oxygen at a cut edge of the sample, where defects are created by the cut (**Figure 2**a). The SEM image from the cut edge reveals intimate contact of the pCN thin film with the substrate surface, which is an important characteristic when it comes to light management applications and preparation of multilayered structures like planar heterojunctions, but also for sheer layer adhesion. The carbon, nitrogen, and silicon EDX elemental mappings show that nitrogen (in green) and carbon (in red) elements (Figure 2b,c) are homogeneously distributed among the pCN thin film. The silicon (Figure 2d) and oxygen (Figure S4, Supporting Information) elemental mappings

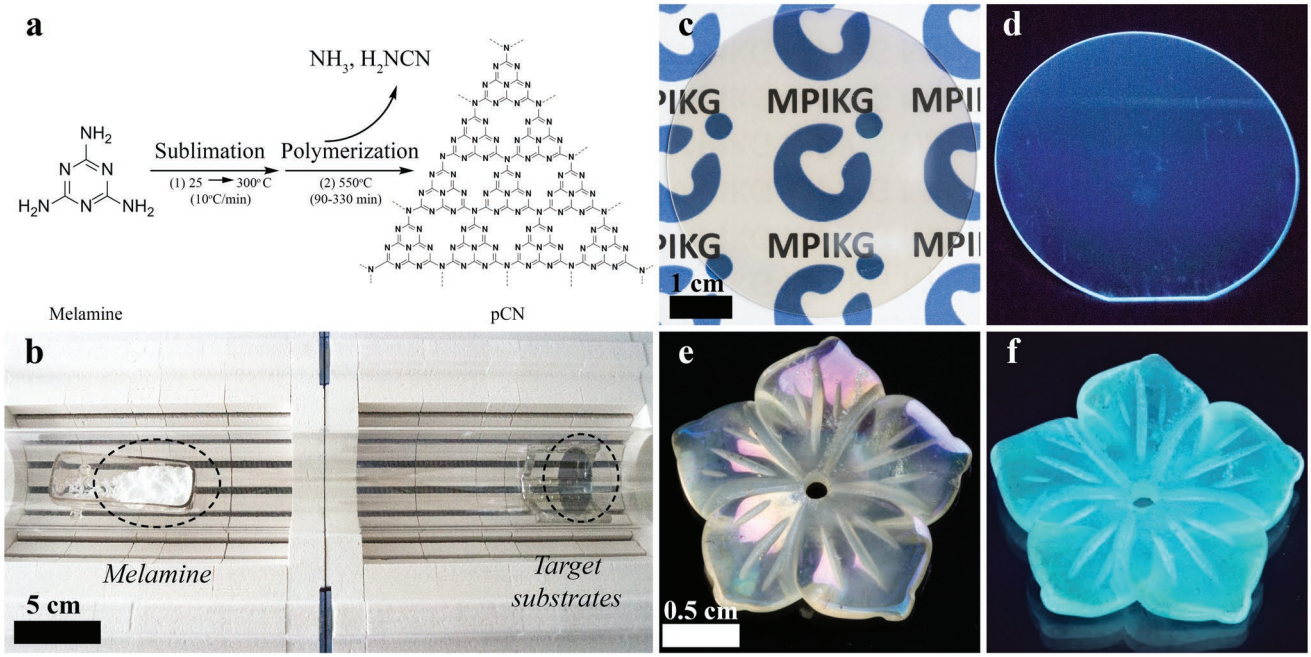

Figure 1. Highly homogenous pCN thin films obtained by CVD. a) Reaction scheme for the synthesis of pCN from melamine. b) Photograph of the CVD setup with the melamine precursor and the target substrates. c,d) Photographs of the pCN thin films deposited on fused silica substrate with a diameter of 2 in. under ambient conditions and under UV (366 nm) illumination, indicating the homogeneity of fluorescence response. e,f) pCN thin films deposited on a flower-shaped quartz substrate under ambient and under UV (366 nm) illumination.

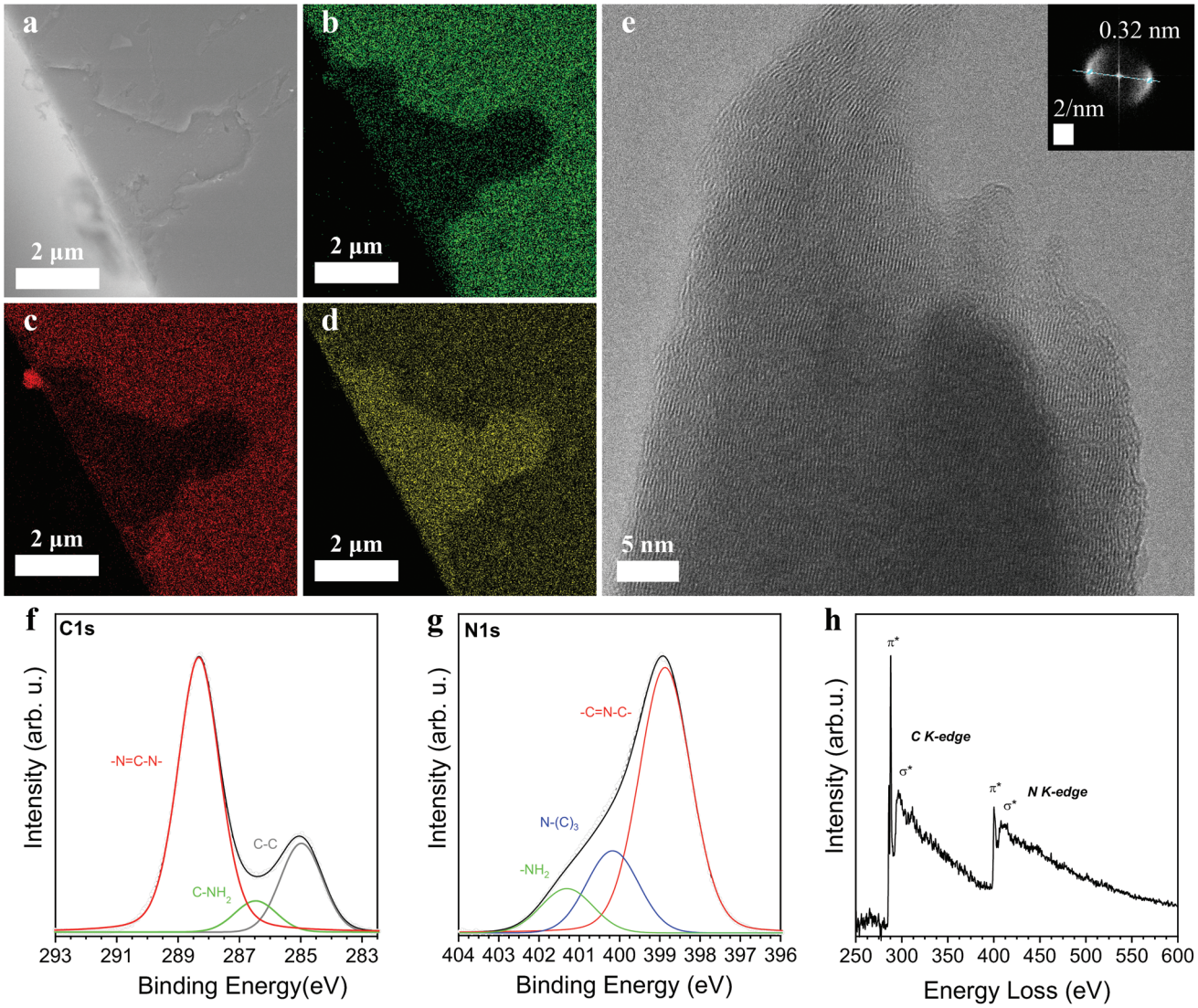

Figure 2. a) SEM image of the pCN thin film on an edge defect created by breaking down the sample. b–d) EDX mapping of nitrogen, carbon, and silicon elements on the pCN thin film at the cut edge. e) TEM image of pCN thin film perpendicular to the in-plane direction. The FFT inset shows the presence of a periodic pattern with an interlayer distance of 0.32 nm. f,g) C 1s and N 1s deconvoluted XPS peaks of pCN thin films. h) EELS core loss spectrum of pCN thin films at the C and N K-edges. The spectrum is shown up to 600 eV in order to highlight the absence of oxygen impurities at about 532 eV.

depict the area in which the film has been scratched away, i.e., the substrate. However, also from the area in which the pCN thin film was removed, low signals of C and N are recorded. This indicates the existence of molecular binding which promotes the very intimate contact between substrate and the pCN.

At the nanoscale, the pCN thin film was investigated by transmission electron microscopy (TEM). Along the growth direction the pCN layered structure, peeled-off films show hexagonal diffraction patterns typical for carbon nitride materials (Figure S5a, Supporting Information).[15] The presence of 2D single layers can be deduced by the extended steps at the material edges, where every shade of gray corresponds to new layers added, as emphasized by arrows (Figure S5b, Supporting Information). At higher magnification and perpendicular to the in-plane direction, the pCN shows a slightly undulated, graphitic-like structure with the sheets oriented parallel to the film surface (Figure 2e). The fast Fourier transform (FFT) pattern obtained from the TEM image (inset Figure 2e) reveals a interlayer distance of 0.32 nm, confirmed also by wide angle X-ray diffraction (WAXD) (Figure S6, Supporting Information), in agreement with the average interlayer stacking of graphitic planes ((002) plane) reported for bulk pCN.[16]

In order to prove that the deposited thin films are indeed constituted by the typical heptazine repeating units of pCN, the samples have been analyzed by X-ray photoelectron spectroscopy (XPS), Fourier-transform infrared (FTIR) spectroscopy, electron energy loss spectroscopy (EELS), and combustion elemental analysis (EA). The deconvolution of the XPS C1s signal leads to three different peaks at 288.3, 286.4, and 284.6 eV (Figure 2f). The highly intense peak at 288.3 eV is

attributed to sp^2 carbon of the heptazine rings (−N=C−N−), whereas the one at 286.4 eV typical for carbon bound to amino terminal groups is very low.[17] The peak at 284.6 eV is attributed to C−C bonds from adventitious carbon, usually unintentionally adsorbed on the pCN thin film surface.[17] The deconvolution of the N1s peak shows the typical heptazinic conjugated nitrogen groups and terminal amino groups at 401.3 eV (Figure 2g). With respect to the conjugated nitrogen atoms, the central heptazinic nitrogen component is found at 400.1 eV, while the intense N-aromatic nitrogen peak appears at 398.2 eV.[17] The chemical structure of the herein presented pCN thin films is in good agreement with previous reports on pCN and is further confirmed by FTIR spectroscopy (Figure S7, Supporting Information). The infrared fingerprint of the pCN thin films reveals the presence of stretching modes of amino terminal groups (3400–3000 cm^{-1}) and the characteristic heptazine breathing mode (804 cm^{-1}), in good agreement with XPS analysis.[16] The carbon-to-nitrogen ratio calculated from XPS analysis of C/N = 0.71 is just slightly lower than the one obtained from EA (0.74), and thus in both cases very close to the ideal value of 0.75 of pCN. The difference in the C/N value points to a minor incomplete condensation within the film. The core-level EELS spectrum of the pCN thin film reveals that carbon (at 288 eV) and nitrogen (at 400 eV) K-edges have very prominent, extremely sharp 1s→π^* peaks which are more intense than the σ^* peak. This confirms the very high degree of unperturbed conjugation of sp^2-hybridized carbon and nitrogen atoms (Figure 2h).[15] Moreover, the nearly identical K-edge structures of carbon and nitrogen atoms indicate a similar electronic environment of the two constituting elements in the pCN thin film.[15] From the comparison with the EELS spectra of many other carbon nitrides in our lab, we can state that this is one of the most organized polymeric carbon nitrides we ever had in our hands. It is worth to notice that the missing oxygen peak (at about 532 eV) confirms the absence of oxygen contamination in the pCN.

The high homogeneity and flatness achieved for the pCN thin films allow for optical applications, which is the central objective of this contribution. Here, the film quality requirements are stricter than in other cases. For instance, undesired scattering effects have to be avoided. The pCN is well known for the typical yellowish appearance due to the absorption edge extending to the very blue region of the visible spectrum (Figure 1c,e). These properties can be qualitatively followed by transmittance and reflectance measurements (Figure S8, Supporting Information). Transmittance spectra of the pCN thin film samples show a steep decrease of the intensity at the blue edge of the visible range due to the onset of pCN absorption. At longer wavelengths, above 450 nm, the transmittance increases, perfectly mirrored by the corresponding evolution of reflectance spectra. Of note, the sum of the spectral intensities of transmittance and reflectance is very close to unity at all wavelengths, which further confirms the high quality of the pCN thin films prepared, as also shown by AFM measurements (Figure S2, Supporting Information).

Moreover, as previously mentioned, the pCN film thickness can be tuned by increasing the amount of melamine precursor and/or changing the synthesis time. By increasing the amount of melamine precursor, the pCN film thickness increases. With longer reaction time, the film thickness decreases, which is attributed to the fact that the reaction is run close to the pCN polymerization/depolymerization point. The high visibility of the interference fringes in the reflectance and transmittance spectra (Figure S8, Supporting Information) reveals that the as-prepared pCN thin films possess a very high refractive index.[18] Therefore, pCN thin films were characterized by variable angle spectroscopic ellipsometry (VASE) which allows for modeling of the real and imaginary part of the complex refractive index over a wide spectral range (**Figure 3**a). pCN absorbs toward the UV range and indeed the extinction coefficient (k) reaches values of 1.97 at 4.1 eV (λ = 301 nm), which is very high compared to other conjugated polymers.[19] High extinction coefficients in polymeric semiconductors are mostly due to a very high density of states and high transition dipole moments and were recently also attributed to high orientation and high stiffness of the polymer chains.[19] The extinction coefficient reveals a pronounced absorption shoulder at about 3.37 eV ($\lambda \approx$ 370 nm) attributed to π–π^* transitions, in good agreement with bulk pCN (Figure S9, Supporting Information) and previous reports on pCN thin films.[20,21] However, we cannot exclude at this stage also a minor contribution to the absorption due to trap states.

The real part of the refractive index n is with values of n_D = 2.43 and still 2.32 at 1000 nm very high as well, following the typical Sellmeier dispersion trend (Sellmeier parameters are reported in Table S1, Supporting Information). To the best of our knowledge, this is the highest ever recorded intrinsic n_D for a polymeric material, and in the reference range even reaching the value of diamond with n_D = 2.42.[12] The typical n_D values of optical polymers with high transparency in the visible spectrum are in the range of 1.33–1.7, and among them high-refractive-index polymers (HIRP) very seldomly exceed 1.8.[10] Semiconductor polymers such as poly(arylenevinylene)s and poly(fluorene)s have typical values of n in the range 1.6–2.1, however, absorbing in a wide range of the visible spectrum.[11] High-n materials with high transparency in the visible range such as the herein presented pCN will open the way to new generation organic photonic devices for enhanced light–matter interaction that up to now has been dominated by inorganic materials, e.g., by crystalline TiO_2 (n_D = 2.5–2.6).[22] The synthesis of HRIP has been thoroughly exploited in the recent years also for optoelectronic devices such as microlenses for charge coupled devices (CCD), complementary metal–oxide–semiconductor (CMOS) image sensor (CIS), and highly efficient light-emitting diode (LED) encapsulants.[10] Indeed, carbon nitride structures may take an interesting share in these applications.

It must be mentioned, that these reported values are retrieved under environmental conditions and in equilibrium with ordinary atmosphere at around 80% relative humidity. pCN has structural pores which indeed might be filled with gases and very small molecules (such as water), thus adding a little on the refractive index. In any case, an explanation for high n values as such has to be attributed to molecular structure of the pCN which is constituted by cross-linked heptazine units. Here, the heteroaromatic −C=N−C− bonds possess higher molar refraction ($[R]$ = 4.1) as compared to the −C=C− bonds ($[R]$ = 1.7), as delineated by the Lorentz–Lorenz equation (Equation (1)):

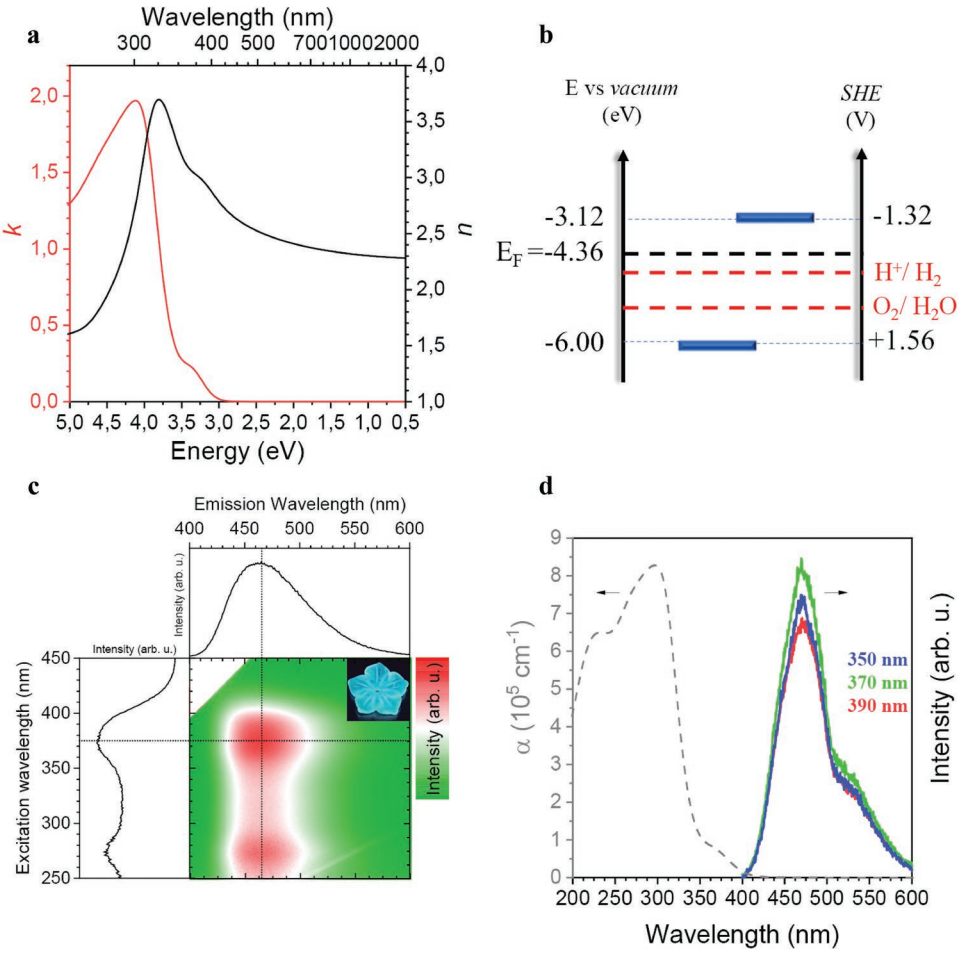

Figure 3. a) Optical functions of pCN thin film: extinction coefficient, *k* (red line), and refractive index, *n* (black line), as a function of energy and wavelength. b) Band structure of pCN thin films with respect to vacuum level (left axes) and SHE (right axes). c) Contour plot of photoexcitation versus photoluminescence spectra of pCN thin films; on the *x*-axis the photoluminescence spectrum at 375 nm excitation is shown, on the *y*-axis the excitation spectrum at 466 nm emission; dotted lines are added to the contour plot to clarify the excitation and emission wavelengths used for the 2D plots; the inset shows the emission color of the pCN thin film on the flower-shaped quartz substrate. d) Long-living emission spectra at different excitation wavelengths: 350 (blue line), 370 (green line), and 390 (red line). The absorption coefficient spectrum (in dashed gray lines) is shown for clarity reasons.

$$\frac{n^2-1}{n^2+2}=\frac{[R]}{V_m} \quad (1)$$

where V_m is the molecular volume of the polymer repeat unit.[10] The combined VASE, reflectance, and transmittance characterization allows also for the determination of the pCN film thicknesses on fused silica substrates. In the present cases, thickness measurements reveal thicknesses ranging between 6 and 130 nm and confirm that this parameter can be tuned by the amount of melamine used as precursor and by the synthesis time (Table S2, Supporting Information).

The unique electronic properties and the highest occupied molecular orbital/lowest unoccupied molecular orbital (HOMO–LUMO) band position of pCN have been the most exploited properties of this semiconductor polymer, so far. The pCN is a polymeric medium-bandgap, indirect semiconductor with a HOMO–LUMO energy gap lying at the edge of the visible spectrum.[23] The elaboration of the absorption coefficient function of the pCN thin films (Figure S10a, Supporting Information) allows for defining the optical bandgap by the Tauc plot method (Figure S10b, Supporting Information). The HOMO–LUMO energy levels of the pCN thin films (Figure 3b) are also accessible by means of ultraviolet photoelectron spectroscopy (UPS) (Figure S11, Supporting Information). The data show, that the pCN thin films are n-type semiconductors, since the Fermi level (E_F, −0.08 V vs standard hydrogen electrode, SHE) lies closer to the LUMO (−1.32 V vs SHE) with respect to the HOMO (+1.56 V vs SHE). The pCN thin films possess a larger bandgap of 2.88 eV as compared to the bulk materials (2.74 eV).[1] The wider bandgap of thin film materials with respect to the bulk states is attributed to a decreased concentration of trap states near the conduction band: indeed, the HOMO energy level is in good agreement with previous reports (+1.57 V), whereas the LUMO level shifts to lower negative values.[1] In this context, we recall that the pCN thin films shown here are poor in contaminants such as oxygen, as the synthesis was conducted at low pressures in nitrogen environment. As the bandgap is independent of film thickness, we can also exclude quantum confinement effects.

The pCN optical characterization and band structure also simplify future implementation of pCN thin films in organic optoelectronic devices such as photo-(electro-)chemical and buffer layer in solar cells devices.[1,2,24,25] Indeed, preliminary periodic on/off photocurrent tests have already shown promising results for pCN thin films in photoelectrochemical cells under visible light (Figure S12, Supporting Information).

The optical bandgap in the violet region of the visible spectrum of pCN thin films is consistent with its yellow color appearance.[2,23] However, to better understand and therefore exploit the light-induced exciton creation and recombination mechanisms, photoluminescence and long-living luminescence spectra were recorded at different wavelengths (Figure 3c,d, Supporting Information). When subjected to UV light stimuli, pCN exhibits intense blue photoluminescence emission with a single maximum at 466 nm (λ_{exc} = 375 nm) (Figure 3c) and with external and internal quantum yields of 0.8% and 1.1% at 370 nm excitation, respectively. The low photoluminescence quantum yield can be attributed to the presence of trap states in carbon nitride materials.[26] Indeed, traps constitute a nonradiative decay pathway competing with the radiative recombination, thus reducing the photoluminescence efficiency. The excitation versus emission contour plot shows that for the peak wavelength of photoluminescence emission, i.e., 466 nm, two main excitation modes with maxima at 275 and 375 nm are present. The two excitation maxima are attributed to π–π^* electronic transitions in pCN thin films, whereas, the lone pair-π^* transition appears as a shoulder at about 394 nm.[20,21] However, the emission processes in pCN are complex and still under debate in the scientific community.[20] The time-resolved fluorescence decay curves (Figure S13, Supporting Information) at 405 nm excitation reveal a strongly nonexponential decay, indicating a broad distribution of lifetimes of the excited electronic states.[27] The distribution of fluorescence lifetimes shows three modes with 2.1, 11.4, and 61.4 ns decay times. The lower lifetimes are in agreement with previous characterizations on pCN lifetimes, usually around 2 and 8–10 ns.[28] The longer lifetime at 61.4 ns is to our opinion related to the high conjugation degree and high orientation achieved in the pCN thin film, as shown by EELS characterization (Figure 2h). The strongly nonexponential decay in pCN was previously attributed to transport of the excitation via resonant energy transfer or hopping of excitons.[27]

Moreover, the occurrence of long-living emission (Figure 3d) reveals once more the complexity of electronic processes in pCN thin films.[26,29] Long-living emission spectra have been recorded with different excitation wavelengths (350, 370, 390 nm) and with a large impulse-detection delay of 10 ms. The spectral shape at different excitation wavelengths appears quite similar. The spectra show a maximum at 470 nm and a broad shoulder above 500 nm. The long-living emission is attributed to the contribution of two mechanisms: delayed singlet fluorescence, due to the presence of trap states, and phosphorescence emission.[26] Indeed, the long-living emission intensity decreases when exposing the pCN thin film to oxygen with respect to nitrogen, which confirms the oxygen sensitivity to phosphorescence emission (Figure S14, Supporting Information). Long-living trapped charges and triplet generation offer further future perspectives in light harvesting for energy-transfer-based photocatalytic processes, which to date has been seldom exploited, as well as for applications in photonic devices, photocatalysis, and bioimaging.[30]

The deposition of pCN was then successfully repeated on many different substrate materials and shapes, still resulting in conformal films, as exemplarily shown by depositing pCN on a glass slide and carbon paper substrates (Figure S15, Supporting Information). Our current selection of substrates included glass, quartz, fused silica, silicon, fluorine-doped tin oxide (FTO), carbon paper, copper, platinum, anodic aluminum oxide (AAO), and even TiO_2 powder, enhancing once more the flexibility and the opportunities for future applications. Moreover, the presented method (with minor modifications) is applicable to other pCN precursors such as cyanamide, dicyanamide, or urea, i.e., the process can be adjusted to the demands of the application.

On top of the extraordinary optical properties, the pCN thin films also show excellent mechanical properties. They are very hard as evaluated by nanoindentation, having a Young's modulus and hardness of 36.5 and 2.2 GPa, respectively (Figure S16, Supporting Information). Notably, these values are higher than those of hard polymer materials such as polyimide and kevlar thin films and, in particular, the Young's modulus is even higher than the glassy carbon with values of which are reported between 20 and 30 GPa.[31] These values are referred perpendicular to the 2D-layer orientation and are thereby especially remarkable. To recall, graphite has a Young's modulus of 4–28 GPa, and hardness of 0.3 GPa, while single-layer graphene (in film direction) exhibits a Young's modulus of ≈900–1000 GPa and hardness of 950 GPa. Both decrease by a factor of ≈3 already for a bilayer.[32] Diamond films are of course stronger: typical values for the Young's modulus are 500–530 GPa, and for the hardness 80–100 GPa.[33] For a CVD film made at only 550 °C, the mechanical performance is, however, already very promising, i.e., the pCN coating does not only possess outstanding optical properties but also offers unexpected mechanical protection against damage.

In summary, we herein presented the synthesis of high-quality polymeric carbon nitride thin films from melamine by thermal chemical vapor deposition. Melamine is a convenient precursor since it can be quantitatively sublimated at a relatively low temperature. The two-chamber CVD technique allows for tuning the pCN thin film thickness by means of synthesis time and/or precursor amount, and the as-grown films are homogeneous even at curved surfaces.

We examined the optical properties of these films, a field which previously was hardly accessible because of the missing transparency and low quality of the previous pCN thin films. We could quantify not only the absorption coefficient of the material ($\alpha = 8.27 \times 10^5$ cm^{-1} at 4.2 eV) but also the refractive index (n_D = 2.43), which is even in the range of diamond. The high quality of the deposition and the outstanding refractive index values are of high interest for the development of highly efficient devices for light management, like photonic crystals, optical fibers, sensors, and nanodevices based on Mie resonance.[13] Moreover, we quantified the band structure and the emission properties, which can provide a reference point for the development of (fully)organic planar heterojunctions and optoelectronic devices which are based on visible light harvesting, like photo-(electro-)chemical cells.[24,34] The organic

structure of and synthesis pathway to pCN offer the opportunity to engineer the optical and electronic properties by simple chemical doping. Therefore, based on the findings reported herein, a more general appearance of carbon-nitride-based materials for thin films-based devices is expected.[1]

Experimental Section

Synthetic Procedure for pCN Thin Films by CVD: The preparation of pCN thin films was conducted with a planarGROW-3S-OS CVD System for Organic Semiconductor, provided by planarTECH, with a 3 in. quartz tube. In a typical recipe, a 2 in. fused silica substrate was placed vertically in the center of the second CVD oven and a glass boat containing melamine (5 g) in the center of the first one, as shown in Figure 1b. Then, the vacuum was pulled down to 10 Torr and the temperature at the substrate was raised to 550 °C, with 50 sccm nitrogen flow as carrier gas. As soon as the substrate was at 550 °C, the melamine was heated up to 300 °C at a rate of 10 °C min^{-1}, and kept for additional 30 min. The substrates were kept for additional 30 min at 550 °C after the first oven heating program was finished. The samples were let cool down naturally and collected at room temperature. Of note, the melamine was in all cases completely consumed during the experiments. A typical growth profile can be found in Figure S17 (Supporting Information).

Scanning Electron Microscopy and Energy-Dispersive X-Ray Spectroscopy: SEM imaging was performed after Au/Pd sputtering of the sample on carbon sample holders in a Zeiss LEO 1550-Gemini system (acceleration voltage: 3 to 10 kV). An Oxford Instruments X-MAX 80 mm^2 detector was used to collect the SEM-EDX data.

Transmission Electron Microscopy and Electron Energy Loss Spectroscopy: The measurements were acquired using a double-Cs-corrected Jeol JEM-ARM200F microscope, equipped with a cold field emission gun, a Gatan GIF Quantum detector, and a JED-2300 energy-dispersive X-ray detector. The acceleration voltage was typically set to 80 kV.

X-Ray Photoelectron Spectroscopy: XPS measurements were performed using CISSY equipment with a SPECS XR 50 X-ray gun Mg Kα radiation (1254.6 eV) and Combined Lens Analyzer Module (CLAM).

Spectroscopic Ellipsometry Characterization: Spectroscopic ellipsometry measurements have been performed by using VASE instrument by J. A. Woollam Co. equipped with rotating analyzer and AutoRetarder in the range 250–2500 nm at different angles of incidence from 55° to 75° at ambient temperature and humidity. Transmittance and reflectance at normal incidence were measured with Varian Cary 6000i spectrometer in the spectral range 200–1800 nm. Measurements and data modeling by WVASE32 software assumed the samples to be isotropic, deriving the optical function, absorption coefficient, and thickness values.

Fluorescence Spectroscopy: Photoluminescence spectra were recorded by Horiba FluoroMax-4 equipped with a thin film sample holder set at 60° with respect to the excitation, integration time 0.2 to 1 s, and slits apertures 1.

Long-Living Emission Spectroscopy: Long-living emission spectra were recorded by a Jasco FP-8300 spectrofluorometer with 10 ms delay, 50 ms chopping time, and 10 nm slits aperture.

Supporting Information

Supporting Information is available from the Wiley Online Library or from the author.

Acknowledgements

The authors thank the Max Planck Society for financial support, Valerio Molinari, Nieves Lopez-Salas, Baris Kumru, and Regina Rothe for the useful discussion and help during the development of this work. The authors are grateful Shahrouz Amini, Reinhild Dünnebacke, and Aleksandr Savateev for the nanoindentation, AFM tests, and photocurrent measurements.

Conflict of Interest

The authors declare no conflict of interest.

Keywords

chemical vapor deposition, optical properties, polymeric carbon nitride, refractive index, thin films

Received: December 11, 2019
Revised: December 21, 2019
Published online: January 29, 2020

[1] S. Cao, J. Low, J. Yu, M. Jaroniec, *Adv. Mater.* **2015**, *27*, 2150.
[2] X. Wang, K. Maeda, A. Thomas, K. Takanabe, G. Xin, J. M. Carlsson, K. Domen, M. Antonietti, *Nat. Mater.* **2009**, *8*, 76.
[3] B. J. Yeh, W. A. Lim, *Nat. Chem. Biol.* **2007**, *3*, 521.
[4] J. Liebig, *Ann. Pharm.* **1834**, *10*, 1.
[5] B. Kumru, M. Antonietti, B. V. Schmidt, *Langmuir* **2017**, *33*, 9897.
[6] W. Xiong, F. Huang, R.-Q. Zhang, *Sustainable Energy Fuels* **2020**, https://doi.org/10.1039/C9SE00785G.
[7] K. Xiao, P. Giusto, L. Wen, L. Jiang, M. Antonietti, *Angew. Chem.* **2018**, *130*, 10280.
[8] J. Bian, C. Huang, R. Q. Zhang, *ChemSusChem* **2016**, *9*, 2723.
[9] H. Arazoe, D. Miyajima, K. Akaike, F. Araoka, E. Sato, T. Hikima, M. Kawamoto, T. Aida, *Nat. Mater.* **2016**, *15*, 1084.
[10] T. Higashihara, M. Ueda, *Macromolecules* **2015**, *48*, 1915.
[11] a) A. Mathy, K. Ueberhofen, R. Schenk, H. Gregorius, R. Garay, K. Müllen, C. Bubeck, *Phys. Rev. B* **1996**, *53*, 4367; b) N. C. Greenham, R. H. Friend, D. D. Bradley, *Adv. Mater.* **1994**, *6*, 491; c) M. Campoy-Quiles, G. Heliotis, R. Xia, M. Ariu, M. Pintani, P. Etchegoin, D. D. Bradley, *Adv. Funct. Mater.* **2005**, *15*, 925.
[12] G. Turri, S. Webster, Y. Chen, B. Wickham, A. Bennett, M. Bass, *Opt. Mater. Express* **2017**, *7*, 855.
[13] a) A. I. Kuznetsov, A. E. Miroshnichenko, M. L. Brongersma, Y. S. Kivshar, B. Luk'yanchuk, *Science* **2016**, *354*, aag2472; b) P. Lova, G. Manfredi, L. Boarino, A. Comite, M. Laus, M. Patrini, F. Marabelli, C. Soci, D. Comoretto, *ACS Photonics* **2015**, *2*, 537; c) M. Maragkou, *Nat. Mater.* **2015**, *14*, 1086.
[14] A. C. Edrington, A. M. Urbas, P. DeRege, C. X. Chen, T. M. Swager, N. Hadjichristidis, M. Xenidou, L. J. Fetters, J. D. Joannopoulos, Y. Fink, *Adv. Mater.* **2001**, *13*, 421.
[15] A. Thomas, A. Fischer, F. Goettmann, M. Antonietti, J.-O. Müller, R. Schlögl, J. M. Carlsson, *J. Mater. Chem.* **2008**, *18*, 4893.
[16] F. K. Kessler, Y. Zheng, D. Schwarz, C. Merschjann, W. Schnick, X. Wang, M. J. Bojdys, *Nat. Rev. Mater.* **2017**, *2*, 17030.
[17] K. Akaike, K. Aoyama, S. Dekubo, A. Onishi, K. Kanai, *Chem. Mater.* **2018**, *30*, 2341.
[18] J. Manifacier, J. Gasiot, J. Fillard, *J. Phys. E: Sci. Instrum.* **1976**, *9*, 1002.
[19] M. S. Vezie, S. Few, I. Meager, G. Pieridou, B. Dörling, R. S. Ashraf, A. R. Goñi, H. Bronstein, I. McCulloch, S. C. Hayes, *Nat. Mater.* **2016**, *15*, 746.
[20] J. Bian, J. Li, S. Kalytchuk, Y. Wang, Q. Li, T. C. Lau, T. A. Niehaus, A. L. Rogach, R. Q. Zhang, *ChemPhysChem* **2015**, *16*, 954.
[21] J. Bian, Q. Li, C. Huang, J. Li, Y. Guo, M. Zaw, R.-Q. Zhang, *Nano Energy* **2015**, *15*, 353.

[22] a) J. R. DeVore, *JOSA* **1951**, *41*, 416; b) S. Ratzsch, E.-B. Kley, A. Tünnermann, A. Szeghalmi, *Nanotechnology* **2014**, *26*, 024003.
[23] Y. Wang, X. Wang, M. Antonietti, *Angew. Chem., Int. Ed.* **2012**, *51*, 68.
[24] a) J. Xu, T. J. Brenner, L. Chabanne, D. Neher, M. Antonietti, M. Shalom, *J. Am. Chem. Soc.* **2014**, *136*, 13486; b) J. H. Heo, S. H. Im, J. H. Noh, T. N. Mandal, C.-S. Lim, J. A. Chang, Y. H. Lee, H.-J. Kim, A. Sarkar, M. K. Nazeeruddin, *Nat. Photonics* **2013**, *7*, 486.
[25] a) M. Volokh, G. Peng, J. Barrio, M. Shalom, *Angew. Chem., Int. Ed.* **2019**, *58*, 6138; b) D. Cruz, J. Garcia Cerrillo, B. Kumru, N. Li, J. Dario Perea, B. V. Schmidt, I. Lauermann, C. J. Brabec, M. Antonietti, *J. Am. Chem. Soc.* **2019**, *141*, 12322.
[26] R. Godin, Y. Wang, M. A. Zwijnenburg, J. Tang, J. R. Durrant, *J. Am. Chem. Soc.* **2017**, *139*, 5216.
[27] C. Merschjann, T. Tyborski, S. Orthmann, F. Yang, K. Schwarzburg, M. Lublow, M.-C. Lux-Steiner, T. Schedel-Niedrig, *Phys. Rev. B* **2013**, *87*, 205204.
[28] H. Zhang, A. Yu, *J. Phys. Chem. C* **2014**, *118*, 11628.
[29] H. Wang, S. Jiang, S. Chen, X. Zhang, W. Shao, X. Sun, Z. Zhao, Q. Zhang, Y. Luo, Y. Xie, *Chem. Sci.* **2017**, *8*, 4087.
[30] a) K. L. Corp, C. W. Schlenker, *J. Am. Chem. Soc.* **2017**, *139*, 7904; b) W. Yang, R. Godin, H. Kasap, B. Moss, Y. Dong, S. A. J. Hillman, L. Steier, E. Reisner, J. R. Durrant, *J. Am. Chem. Soc.* **2019**, *141*, 11219.
[31] J. Bauer, A. Schroer, R. Schwaiger, O. Kraft, *Nat. Mater.* **2016**, *15*, 438.
[32] Y. Zhang, C. Pan, *Diamond Relat. Mater.* **2012**, *24*, 1.
[33] N. Savvides, T. Bell, *Thin Solid Films* **1993**, *228*, 289.
[34] J. Bian, L. Xi, C. Huang, K. M. Lange, R. Q. Zhang, M. Shalom, *Adv. Energy Mater.* **2016**, *6*, 1600263.